Mössbauer, Electron Spin Resonance, Optical, and Magnetic Studies of Iron(III) in Oxide Host Lattices

By **T. Birchall** † and **N. N. Greenwood,** * Department of Inorganic Chemistry, University of Newcastle upon Tyne, NE1 7RU
A. F. Reid, Division of Mineral Chemistry, C.S.I.R.O., Melbourne, Australia

Spectroscopic and magnetic studies have been made on Fe^{3+} ions in a variety of oxide host lattices, namely $NaSc_{1-x}Fe_xTiO_4$, $NaFeSnO_4$, $CaSc_{2-x}Fe_xO_4$, $Sc_{2-x}Fe_xTiO_5$, $NaFeTi_3O_8$, α-$NaSc_{1-x}Fe_xO_2$, $Cs_xSc_{x-y}Fe_yTi_{2-x}O_4$, β-$NaAl_{1-x}Fe_xO_2$, $Cs_xSc_{x-y}Fe_yTi_{1-x}O_8$, $LiFeTiO_4$, and $CsFeSi_2O_6$. The ^{119}Sn Mössbauer spectra of $NaFeSnO_4$ and $NaScSnO_4$ were also recorded. In most of these lattices the crystal fields at the iron sites depart significantly from cubic symmetry and we have found that isolated Fe^{3+} ions give rise to a strong e.s.r. signal at $g' = 4{\cdot}3$ and a magnetic Mössbauer spectrum. These spectra are strongly concentration and temperature dependent. We conclude that the magnetic Mössbauer spectra are the result of a pure spin-alignment effect, while the $g' = 4{\cdot}3$ e.s.r. signal is the result of ground-state splitting which occurs even when the spins are not strictly aligned. The electronic spectra of these compounds have been analysed and the bands corresponding to a particular transition are found to be remarkably constant. Only those transitions which correspond to the two lowest levels, and whose energies are crystal-field dependent, show significant changes in band position.

In a recent investigation of the solid-solution series $NaScTiO_4$–$NaFeTiO_4$ it was found that at low Fe^{3+} concentrations a sharp e.s.r. absorption at $g' = 4{\cdot}27$ was obtained, a characteristic of isolated Fe^{3+} ions in a rhombic crystal field.[1] At higher concentrations this line was replaced by one at $g' = 2{\cdot}00$, an effect attributable to superexchange coupling between pairs of Fe^{3+} ions linked by oxygen atoms. The optical absorption spectra also showed marked changes as the Fe^{3+} concentration increased. Although the members of the series all showed paramagnetism, at least above 77°K, the Weiss temperature showed a strong increase with concentration of Fe^{3+}, while the effective magnetic moment decreased significantly from the spin-only value, behaviour indicative of limited antiferromagnetic coupling. Mössbauer data for this system showed a quadrupole-split Fe^{3+} absorption for Fe^{3+}/Sc^{3+} ratios above 0·1. At lower concentrations however the results

† *Present address:* Department of Chemistry, McMaster University, Hamilton, Ontario, Canada.

[1] A. F. Reid, H. K. Perkins, and M. J. Sienko, *Inorg. Chem.*, 1968, **7**, 119.

were inconclusive, primarily because the Mössbauer isotope, ^{57}Fe, is only 2·2% naturally abundant, and the γ-ray absorption was consequently too slight for accurate measurement.

In the present work we have investigated the low Fe^{3+} region with samples containing iron enriched to 91% in ^{57}Fe, and found at 77°K a (partially collapsed) six-line pattern normally characteristic of Fe^{3+} in a ferromagnetic environment. Such a six-line Mössbauer spectrum for Fe^{3+}, together with an e.s.r. line at $g' = 4{\cdot}27$, have previously been mentioned for ferrichrome A, a cyclic hexapeptide containing Fe^{3+} co-ordinated by way of six oxygen atoms to the large organic moiety.[2] While each Fe^{3+} is completely isolated, the arrangement of ligands is such that each Fe^{3+} is placed in a strong rhombic crystal field.

To enlarge on the apparent connection between these two sets of observations we have attempted to determine whether magnetic Mössbauer spectra as well as anisotropic g' values are typical of Fe^{3+} ions in rhombic or axial crystal field symmetries. In order to determine which effects are due to isolated Fe^{3+} ions and which to superexchange or magnetic coupling, we have examined the e.s.r., Mössbauer, and optical spectra and the magnetic susceptibilities of several series of isomorphous compounds in which Fe^{3+} progressively replaces Al^{3+} or Sc^{3+}.

Of the systems listed in Table 1 it will be noticed that the two groups of compounds $NaFeO_2$, $NaFeTiO_4$, $NaFeTi_3O_8$; and $Cs_xFe_xTi_{2-x}O_4$, $Cs_xFe_xTi_{4-x}O_8$ represent major members of the respective phase diagrams for the pseudo-binary systems $NaFeO_2$–TiO_2 and $CsFeO_2$–TiO_2. These oxide host lattices and their scandium-based isomorphs were chosen to have significantly large

TABLE 1

Summary of oxide systems studied

System end members	Mössbauer ion	Average environmental bond length, (Å) [a]	Structure type	Lattice parameters (Å) a	b	c	Z	Space group	Ref. [b]
$NaScTiO_4$–$NaFeTiO_4$	Octahedral Fe^{3+}	2·04	Calcium	9·277	3·048	10·917	4	*Pnma*	3; 1
		2·01	ferrite	9·175	2·962	10·741	4	*Pnma*	3; 1
$CaSc_2O_4$–$CaFe_2O_4$	Octahedral Fe^{3+}	2·12	Calcium	9·460	3·138	11·110	4	*Pnma*	4; 5
		2·03	ferrite	9·217	3·018	10·702	4	*Pnma*	6, 7, 8; 5
$NaScSnO_4$–$NaFeSnO_4$	Octahedral Fe^{3+} and Sn^{4+}	2·09	Calcium	9·466	3·139	11·177	4	*Pnma*	3; 3
		2·05	ferrite	9·347	3·067	11·000	4	*Pnma*	3; 3
Sc_2TiO_5 [c]–Fe_2TiO_5	Octahedral Fe^{3+}	2·06	Pseudo-	3·85	10·15	10·30	4	*Cmcm*	9; 9
		1·99	brookite	3·717	9·767	9·947	4	*Cmcm*	10, 11; 12
$NaFeTi_3O_8$ [d]	Octahedral Fe^{3+}	1·98	Sodium titanium bronze	12·269	3·814	6·488	2	*C2/m*	13, 14, 15; *e*
$NaScO_2$–α-$NaFeO_2$	Octahedral Fe^{3+}	2·12	α-$NaFeO_2$	3·162		16·27	3	$R\bar{3}m$	16; 16
		2·03		3·019		16·09	3	$R\bar{3}m$	17; *e*
β-$NaAlO_2$–B-$NaFeO_2$	Tetrahedral Fe^{3+}	1·76(T)	β-$NaFeO_2$	5·376	7·075	5·216	4	$Pna2_1$	18, 19; 18
		1·86(T)		5·672	7·136	5·377	4	$Pna2_1$	19, 20; 19
$Cs_xSc_xTi_{2-x}O_4$–$Cs_xFe_xTi_{2-x}O_4$	Octahedral Fe^{3+}	2·02	Rb_xMn_x	3·857	17·254	3·035	2	*Imm*2	21; 21
		1·99	$Ti_{2-x}O_4$	3·805	17·102	2·972	2	*Imm*2	21; 21
$Cs_xSc_xTi_{4-x}O_8$–$Cs_xFe_xTi_{4-x}O_8$	Octahedral Fe^{3+}	1·99	Hollandite	10·319		2·984	2	*I*4/*m*	22, *e*; *e*
		1·97		10·278		2·968	2	*I*4/*m*	22, 23, *d*; *e*
$LiFeTiO_4$	Octahedral and tetrahedral Fe^{3+}	2·00	Spinel	8·355			8	*Fd*3*m*	24; *e*
		1·92(T)							
$CsFeSi_2O_6$	Tetrahedral Fe^{3+}	1·70(T)	Pollucite	13·81			16	*Ia*3*d*	25, 26; *e*

[a] Average octahedral or tetrahedral bond length for the host lattice site in which Fe^{3+} is contained. For calcium ferrite and pseudobrookite isomorphs and for β-$NaFeO_2$ bond lengths were obtained using fractional atomic co-ordinates. The remainder were obtained from ' best ' values of bond lengths assembled by R. D. Shannon and C. T. Prewitt (*Acta Cryst.*, 1969, B25, in the press) with appropriate averaging for the proportions of each kind of ion occupying the lattice sites. [b] Structure references, followed after the semicolon by lattice-parameter references. [c] Stabilised with 10 mole% of Fe_2TiO_5. [d] Monoclinic, $\beta = 107{\cdot}24°$. [e] This work.

[2] H. H. Wickman, M. P. Klein, and D. A. Shirley, *J. Chem. Phys.*, 1965, **42**, 2113.
[3] A. F. Reid, A. D. Wadsley, and M. J. Sienko, *Inorg. Chem.*, 1968, **7**, 112.
[4] H. Müller-Buschbaum and H. G. Schnering, *Z. anorg. Chem.*, 1965, **336**, 259.
[5] A. F. Reid, *Inorg. Chem.*, 1967, **6**, 631.
[6] E. F. Bertaut, P. Blum, and G. Magnano, *Bull. Soc. France Minér. Crist*, 1956, **129**, 536.
[7] P. M. Hill, H. S. Peiser, and J. R. Rait, *Acta Cryst.*, 1956, **9**, 981.
[8] B. F. Decker and J. S. Kasper, *Acta Cryst.*, 1957, **10**, 332.
[9] W. Mumme and A. F. Reid, to be published.
[10] L. Pauling, *Z. Krist*, 1930, **73**, 97.
[11] M. Hamelin, Proceedings 16th I.U.P.A.C. Meeting, Paris, 1957, Butterworths, London, 1958, p. 151.
[12] S. Akimoto, T. Nagata, and T. Katsura, *Nature*, 1957, **179**, 37.
[13] S. Andersson and A. D. Wadsley, *Acta Cryst.*, 1962, **15**, 201.
[14] G. Bayer and W. Hoffman, *Z. Krist.*, 1965, **121**, 9.
[15] A. F. Reid and M. J. Sienko, *Inorg. Chem.*, 1967, **6**, 321.
[16] R. Hoppe, B. Schepers, H. J. Röhrborn, and E. Vielhaber, *Z. anorg. Chem.*, 1965, **339**, 130.
[17] S. Goldsztaub, *Compt. rend.*, 1933, **196**, 280.
[18] J. Théry, D. Briançon, and R. Collongues, *Compt. rend.*, 1961, **252**, 1475.
[19] F. Bertaut and P. Blum, *Compt. rend.*, 1954, **239**, 429.
[20] H. Wanatabe and F. Fukase, *J. Phys. Soc., Japan*, 1961, p. 1181.
[21] A. F. Reid, W. G. Mumme, and A. D. Wadsley, *Acta Cryst.*, 1968, *B***24**, 1228.
[22] A. Bystrom and A. M. Bystrom, *Acta Cryst.*, 1950, **3**, 146.
[23] G. Bayer and W. Hoffman, *Amer. Min.*, 1966, **51**, 511.
[24] G. Blasse, *J. Inorg. Nuclear Chem.*, 1963, **29**, 230.
[25] R. E. Newnham, *Amer. Min.*, 1967, **52**, 1515.
[26] S. Kume and M. Koizumi, *Amer. Min.*, 1965, **50**, 587.

departures from cubic crystal field symmetry at the Fe^{3+} substitution sites. Among the isomorphous series and individual compounds studied, a number of pronounced effects have been observed which result in turn from the interactions of isolated Fe^{3+} ions with their local crystal field environment and with one another.

EXPERIMENTAL

Preparation of Compounds.—The compounds examined were made by powder reactions, usually in open platinum dishes, with particular attention in the case of solid solution compositions to repeated grinding and firing to ensure homogeneity. Starting materials included Sc_2O_3 (99·5%; obtained from the Bureau of Mines, South Australia), Fe_2O_3 (Fisher Certified Reagent grade), sodium oxalate, lithium carbonate, and recrystallized caesium nitrate (all of analytical reagent grade), and TiO_2 (anatase form) (Fisher Certified Reagent grade). Aluminates were made using high purity amorphous aluminium hydroxide, and silicates using high purity precipitated silica.

Except for $NaScSnO_4$, heated to 1300° for 40 hr. in a sealed platinum capsule, preparations containing the alkali metals were usually heated for 20-hr. periods at 1000°. α-$NaFeO_2$ was however prepared at 600° to prevent its conversion to the β-form. The calcium compounds were prepared at 1200 to 1400°, the higher temperatures being used for the higher scandium contents. The Sc_2TiO_5–Fe_2TiO_5 series was prepared at 1200—1300°. More detailed preparative procedures are described in the references given in Table 1. In each case the compound obtained was characterized by its *X*-ray powder diffraction pattern. Single phases of the appropriate structure were obtained in all the preparations, except in the β-$NaAlO_2$–β-$NaFeO_2$ system, where compositions near 1 : 1 apparently separated into an aluminium-rich and an iron-rich phase each, however, with the β-$NaAlO_2$ structure. Preparations nearer to the end members appeared to be single phase, both by *X*-ray powder diffraction, and by examination under the microscope.

Preparation of Compounds Containing ^{57}Fe.—To ensure uniform distribution of low concentrations of ^{57}Fe in scandium-containing host lattices, an accurately weighed quantity of ^{57}Fe metal was first dissolved in 2N-nitric acid. By means of a calibrated hypodermic syringe, 0·2 to 0·5 ml. quantities of this solution were then transferred onto a weighed quantity of the appropriate composition which had been prefired, finely ground, and slurried in alcohol or acetone. After admixtures with the nitrate solution and careful evaporation to dryness, the preparation was heated at 400° to decompose residual nitrates, finely ground, and then heated at 1000°.

Mössbauer Spectra.—The Mössbauer spectra were recorded either on a drive system which has already been described [27] or on a commercial instrument manufactured by N.S.E.C. of Pittsburg. The temperatures at which the low-temperature Mössbauer data were recorded were not measured and are the temperatures of the coolants used, *i.e.*, liquid nitrogen and liquid helium. Chemical shifts for ^{57}Fe are quoted with respect to the centre of the sodium nitroprusside doublet taken as zero; values for ^{119}Sn are referred to SnO_2.

All spectra, except those obtained from the samples containing very low concentrations of iron ($x = 0{\cdot}01$), were analyzed by a least-squares fit computer programme already described.[28]

Other Measurements.—Magnetic susceptibilities as a function of temperature and field strength were measured for powder samples in a Gouy balance arrangement. Quartz sample-tubes with a diamagnetism observed to be constant with temperature were used, and corrections for tube and host lattice diamagnetism were applied before the calculation of gram-atom susceptibilities. Values of atomic diamagnetism used in these corrections were taken from König.[29]

Electronic absorption spectra in the u.v., visible and near-i.r. regions were obtained as diffuse reflectance spectra in a double-beam Beckman DK-2A spectrophotometer fitted with a reflectance sphere. The appropriate isomorphous scandium- or aluminium-containing end member host lattice was used as a reference sample for the various iron-containing compositions.

E.s.r. spectra were obtained from powdered samples in a standard 9 GHz microwave spectrometer employing 100 kHz modulation. The g' values given in the text and in Table 3 are experimentally defined by $g' = h\nu/\beta H$, where h is the Planck constant, ν the microwave frequency (9·015 kHz), β the Bohr magneton, and H the applied magnetic field.

RESULTS

The oxide systems studied are listed in Table 1. In each case solid solutions between the isomorphous end members were examined, and the Mössbauer parameters obtained as a function of iron concentration are given in Table 2. For 1% or less of Fe replacing Sc or Al, iron enriched to 91% in ^{57}Fe was used.

The e.s.r. results for each of the systems are collected in Table 3, and magnetic susceptibilty data are given in Table 4. Structures and results, including optical spectra, are discussed for each of the compounds or isomorphous series in turn, and a general comparison is made at the end of the paper.

(1) $NaSc_{1-x}Fe_xTiO_4$.—The $NaSc_{1-x}Fe_xTiO_4$ system has been shown to have the $CaFe_2O_4$ structure,[3] with Sc^{3+}, Fe^{3+}, and Ti^{4+} randomly substituted in the available sites, which are of two crystallographic kinds. With unit-cell dimensions $a = 9{\cdot}277$, $b = 3{\cdot}048$, and $c = 10{\cdot}917$ Å, and all atoms in planes at $y = \frac{1}{4}$ and $y = \frac{3}{4}$, the structure has a framework consisting of pairs of crystallographically equivalent metal-oxygen octahedra edge-sharing to produce 'double blocks' with a *b*-axis repeat distance of 3·048 Å, the octahedral edge length and oxygen–oxygen separation. The resulting double chains of edge-sharing octahedra are corner joined to four other double chains containing metal atoms in the second set of crystallographic sites, in the arrangement shown in Figure 1. The sodium atoms are held in linear 'tunnels', with a sodium–sodium separation of

[27] J. D. Cooper, T. C. Gibb, N. N. Greenwood, and R. V. Parish, *Trans. Faraday Soc.*, 1964, **40**, 2097.
[28] B. J. Duke and T. C. Gibb, *J. Chem. Soc.* (*A*), 1967, 1478.
[29] E. König, 'Magnetic Properties of Co-ordination and Organometallic Transition Metal Compounds,' Landolt-Börnstein, New Series, vol. 2, Edited, K. H. Hallwege, Springer-Verlag, Berlin, 1966.

3·048 Å. Each transition-metal ion in the three-dimensional structural framework edge-shares through pairs of oxygen atoms to four other metal atoms at a separation of 3·048 to 3·114 Å (in $NaScTiO_4$), and through one oxygen atom to two further metal atoms in the adjacent double-chain.

TABLE 2

Mössbauer parameters for iron oxide systems

Compound	Temp. (°K)	Chemical shift (mm./sec.)	Quadrupole splitting (mm./sec.)	Magnetic field (kgauss)
$NaSc_{1-x}Fe_xTiO_4$				
$x = 0.01$	77	0·77	—	510
0·02	295	No detectable absorption		
0·05	295	0·64	0·70	
0·10	295	0·67	0·64	
0·25	295	0·68	0·61	
0·50	295	0·68	0·61	
0·75	295	0·66	0·54	
1·00	295	0·69	0·45	
	77	0·81	0·48	
	4·2	0·70	0·00	450
$NaSc_{1-x}Fe_xSnO_4$				
$x = 0.00$	295	0·13(^{119}Sn)	0·00	
1·00	295	0·17(^{119}Sn)	0·00	
	295	0·65(^{57}Fe)	0·50	
$CaSc_{2-x}Fe_xO_4$				
$x = 0.01$	77	0·77		530
0·20	295	0·64	0·59	
	77	0·76	0·60	
1·00	295	0·65	0·45	
		0·65	0·82	
	77	0·76	0·44	
		0·76	0·83	
2·00	295	0·64	0·33	
		0·64	0·74	
	77	0·72	0·00	460
$Sc_{2-x}Fe_xTiO_5$				
$x = 0.01$	77	0·73		520
0·10	295	0·64	0·75	
1·00	295	0·65	0·75	
	77	0·76	0·76	
	4·2	0·77	0·79	
2·00	295	0·66	0·69	
	77	0·80	0·68	
	4·2	0·92		450
$NaFeTi_3O_8$				
	295	0·64	0·38	
	77	0·74	0·39	
α-$NaSc_{1-x}Fe_xO_2$				
$x = 0.005$	77	0·68		540
0·10	295	0·67	0·53	
	77	0·79	0·53	
0·50	350	0·60	0·51	
	295	0·66	0·52	
	77	0·75	0·52	
1·00	295	0·63	0·48	
	77	0·74	0·45	
$Cs_xSc_{x-y}Fe_yTi_{2-x}O_4$				
$x = 0.67$; $y = 0.01$	77	0·6		*ca.* 480
0·20	295	0·64	0·80	
0·67	295	0·63	0·73	
	77	0·74	0·72	
β-$NaAl_{1-x}Fe_xO_2$				
$x = 0.01$	295	0·52		490
	77	0·53		500
0·10	295	0·43	0·26	
	77	0·52	0·32	
0·50	295	0·44	0	430
0·90	295	0·45	$\xi = 0.05$	490
1·00	295	0·44	$\xi = 0.05$	490

TABLE 2 (*Continued*)

Compound	Temp. (°K)	Chemical shift (mm./sec.)	Quadrupole splittihg (mm./sec.)	Magnetic field (kgauss)
$Cs_xSc_{x-y}Fe_yTi_{4-x}O_8$				
$x = 0.63$; $y = 0.01$	77	*ca.* 0·6		*ca.* 530
$x = 0.63$; $y = 0.20$	295	0·69	0·46	
	77	0·82	0·43	
$x = 0.70$; $y = 0.70$	295	0·68	0·46	
	77	0·80	0·44	
$LiFeTiO_4$ *				
(*a*)	295	0·56	0·47	0
	77	0·67	0	460
		0·55	0	430
(*b*)	295	0·56	0·48	0
	77	0·71	0	470
		0·59	0	430
(*c*)	295	0·56	0·48	0
$CsFeSi_2O_6$				
	295	0·47	0·51	

* (*a*) Prepared by heating reactants for 20 hr. at 1000°; (*b*) Prepared from Li_2CO_3 dried at 300°, reactants heated to 1000° and finally 6 hr. at 1050°; (*c*) As for (*b*) followed by annealing at 500° overnight.

TABLE 3

g′ Values for e.s.r. absorption by Fe^{3+} in various oxide host lattices

Host lattice	*g*′	Approximate line width, (gauss) [a]	Qualitative intensity
$NaSc_{1-x}Fe_xTiO_4$ [1] (Calcium ferrite structure)			
$x = 0.01$	4·27 ± 0·02	150	s
$x = 0.10$	4·27 ± 0·02	150	ms
	2·00 ± 0·01	1600	s
	1·95 ± 0·01	60	m
$x = 0.25$	2·00 ± 0·01	1600	s
$NaFeTi_3O_8$ [15]	2·00 ± 0·01	400	s
α-$NaSc_{1-x}Fe_xO_2$ (α-$NaFeO_2$ structure)			
$x = 0.02$	32 ± 1	60	s
	12·1 ± 0·5	100	m
	7·7 ± 0·3	300	m
	4·74 ± 0·2	250	ms
	4·29 ± 0·1	250	ms
	3·39 ± 0·02	100	s
	2·28 ± 0·01	200	vs
	2·03 ± 0·02	150	mw
	1·99 ± 0·02	150	mw
	1·56 ± 0·02	150	mw
	1·49 ± 0·02	150	mw
	1·45 ± 0·02	150	mw
$x = 0.10$	3·39 ± 0·05	100	w
	2·28 ± 0·02	200	w
	2·00 ± 0·01	350	s
$x = 0.50$	2·00 ± 0·01	300	s
$x = 1.00$	2·00 ± 0·01	100	s
β-$NaAl_{1-x}Fe_xO_2$ (β-$NaAlO_2$ structure)			
$x = 0.02$	4·30 ± 0·02	120	ms
	3·75 ± 0·02	150	ms
	2·10 ± 0·01	1000	vs
$x = 0.30$	2·020 ± 0·005	300	s
$Cs_xSc_{2-y}Fe_yTi_{2-x}O_4$ ($Rb_xMn_xTi_{2-x}O_4$ structure)			
$x = 0.67$, $y = 0.02$	4·34 ± 0·05	200	vs
	2·05 ± 0·01	300	m
$x = 0.67$, $y = 0.67$	2·06 ± 0·01	450	vs
$Cs_xSc_{x-y}Fe_{y+1-x}O_8$ (Hollandite structure)			
$x = 0.63$, $y = 0.05$	4·45 ± 0·05	170	s

[a] Line width is taken as the peak to peak separation of the recorded derivative of the absorption. This corresponds to the distance between the steepest positive and negative slopes of the absorption peak, and thus approximately to absorption peak width at half height.

While the sites in alternate double-chains are crystallographically non-equivalent, bond lengths and angles are almost identical for both, a consequence of Sc^{3+}, Fe^{3+}, and Ti^{4+} being substituted randomly into the two kinds of sites. Thus e.s.r. spectra and Mössbauer spectra show only one kind of site environment for Fe^{3+} in $NaSc_{1-x}Fe_xTiO_4$, while two distinct environments can be distinguished for Fe in $CaFe_2O_4$ [30-32] or a few percent of Fe in $CaSc_2O_4$.[33]

$NaSc_{1-x}Fe_xTiO_4$, which exhibited a very strong line at $g' = 4{\cdot}27$ for $x = 0{\cdot}01$ to $0{\cdot}05$. Above $x = 0{\cdot}05$ however this line faded and was replaced by one at $g' = 2{\cdot}00$, attributable to superexchange coupled Fe^{3+}–Fe^{3+} pairs, presumably interacting through two oxygen atoms octahedrally edge-shared. The effects of crystal-field asymmetry were thus removed by this interaction. Optical spectra showed a corresponding strong change in the relative intensities of the electronic transitions.

TABLE 4

Paramagnetic constants for Fe^{3+} in oxide lattices $\chi_{(\text{per gram-atom of } Fe^{3+})} = C/(T + \theta)$ c.g.s. units

Compound	Fraction of octahedral [a] sites occupied by Fe^{3+}	C	θ	μ_{eff} (B.M.) [b]	Temperature range [c] (°K)
$NaSc_{1-x}Fe_xTiO_4$ [1]					
$x = 0{\cdot}01$	0·005	$4{\cdot}401 \pm 0{\cdot}050$	$16{\cdot}5 \pm 2$	5·93	80—370
$x = 0{\cdot}10$	0·050	$4{\cdot}188 \pm 0{\cdot}038$	$25{\cdot}4 \pm 2$	5·79	200—370
$x = 0{\cdot}50$	0·025	$3{\cdot}953 \pm 0{\cdot}047$	125 ± 2	5·62	200—370
$x = 1{\cdot}00$	0·500	$4{\cdot}112 \pm 0{\cdot}030$	270 ± 2	5·73	270—370
$CaFe_2O_4$ [39]	1·000	3·61	580	5·37	500—900
$NaFeTi_3O_8$ [15]	0·250	$4{\cdot}052 \pm 0{\cdot}035$	121 ± 3	5·73	200—370
$NaSc_{1-x}Fe_xO_2$ [d]					
$x = 0{\cdot}10$	0·100	$3{\cdot}526 \pm 0{\cdot}053$	$18{\cdot}8 \pm 4$	5·32	125—370
$x = 0{\cdot}50$	0·500	$4{\cdot}110 \pm 0{\cdot}050$	$-27{\cdot}4 \pm 4$	5·73	250—370
$x = 1{\cdot}00$	1·000	$3{\cdot}84 \pm 0{\cdot}14$	$-53{\cdot}4 \pm 9$	5·55	200—370
$Cs_{0{\cdot}7}Fe_{0{\cdot}7}Ti_{1{\cdot}3}O_4$ [d]	0·350	$3{\cdot}628 \pm 0{\cdot}054$	$132{\cdot}7 \pm 6$	5·39	180—370
$CsFeSi_2O_6$ [d]	0·333	$2{\cdot}272 \pm 0{\cdot}027$	$71{\cdot}6 \pm 4$	4·26	120—370

[a] Tetrahedral sites in $CsFeSi_2O_6$. [b] Calculated from $\mu_{eff} = 2{\cdot}828\,C^{\frac{1}{2}}$. [c] Range over which Curie law was observed to be obeyed. [d] This work.

From Figure 1 it can be seen that although each double block has a similar entity above and below it in the *b*-axis direction, the four faces of the chains of double blocks are in proximity to sodium ions, and a strongly

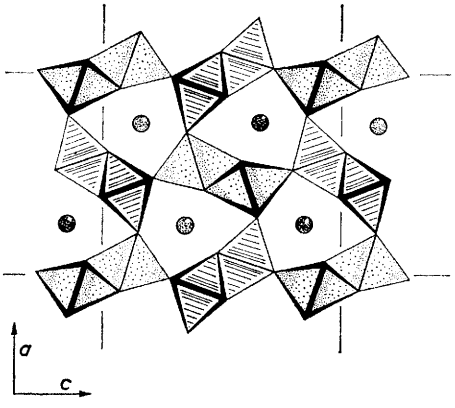

FIGURE 1 The $NaScTiO_4$ structure projected down the 3Å *b*-axis. Lightly marked octahedra contain metal atoms lying at $y = b/4$ in planes parallel to the page and separated by $b/2$ from those heavily marked. Where octahedra are edge or corner joined they have oxygen atoms in common. Stippled and shaded octahedra represent the two crystallographically distinct sets of metal atom sites. Sodium atoms are represented by circles, heavily marked at $y = b/4$ and lightly marked at $y = 3b/4$.

anisotropic crystal field is to be expected at the metal-atom sites. This was confirmed in a previous study [1] by the e.s.r. spectrum of low concentrations of Fe in

Mössbauer parameters at the higher Fe concentrations showed some systematic changes, but at low concentrations were inconclusive.

The present, more complete, Mössbauer investigation yielded the results set out in the Table 2. The values for the chemical shift and quadrupole splitting parameters are characteristic of Fe^{3+} in a somewhat asymmetric environment. Agreement between our data and that reported earlier for the compositions $x = 0{\cdot}1$, $0{\cdot}25$, and $1{\cdot}00$ is excellent. Little change in chemical shift occurs from $x = 1{\cdot}0$ to $x = 0{\cdot}05$ but there is a significant increase in quadrupole splitting indicating that the iron site is becoming more distorted. At $x = 0{\cdot}02$ no meaningful spectra could be observed, and the composition $x = 0{\cdot}01$ was therefore examined with iron enriched in ^{57}Fe. The spectra obtained are shown in Figure 2. At room temperature the central portion of the spectrum (Figure 2a) resembles closely that reported earlier [1] but the wings extend over a considerable velocity range. Apparently similar spectra have been observed for other iron(III) compounds and are attributed to magnetic hyperfine interactions which are partially narrowed by electron spin–spin relaxation.[34] Such spectra are independent of temperature and depend only on the iron–iron distance. Our spectrum is, however, somewhat temperature dependent with the wings sharpening up to show the outer four lines of a six-line pattern as the temperature is lowered (Figure 2b). Presumably the full six-line pattern would be observed

[30] E. F. Bertaut, J. Chappert, A. Apostolov, and V. Semenov, *Bull. Soc. France Minér. Cryst.*, 1966, **89**, 206.
[31] A. Hudson and H. J. Whitfield, *J. Chem. Soc.* (*A*), 1967, 376.
[32] A. Yamamoto, T. Okada, H. Wanatabe, and M. Fukase, *J. Phys. Soc. Japan*, 1968, **24**, 275.
[33] H. K. Perkins, personal communication.
[34] J. W. G. Wignall, *J. Chem. Phys.*, 1966, **44**, 2462.

at still lower temperatures. Collapse of the spectrum is being brought about by spin–spin or possibly spin–lattice relaxation. We estimate the magnetic field at the iron nucleus to be 510 kgauss. This value is close to the expected value for octahedral Fe^{3+} (ref. 35) and

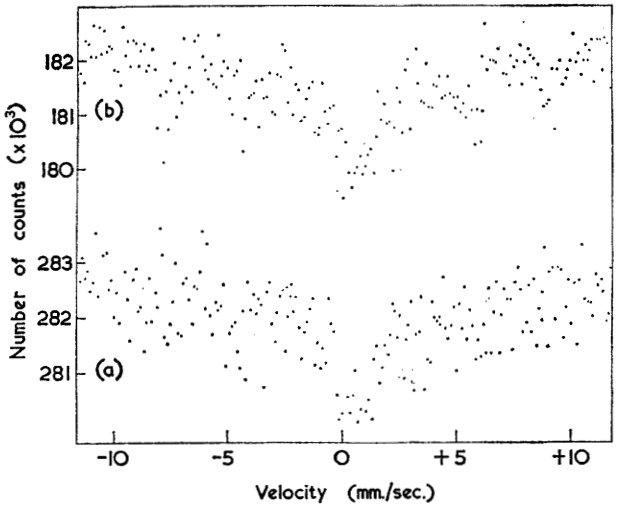

FIGURE 2 Mössbauer spectra of $NaSc_{1-x}Fe_xTiO_4$ ($x = 0{\cdot}01$) at (a) 295°K and (b) 77°K

somewhat larger than that observed for $NaFeTiO_4$ ($x = 1$), for which a fully resolved six-line spectrum was observed at liquid-helium temperatures (Figure 3). At intermediate concentrations ($x = 0{\cdot}10$ to $x = 0{\cdot}75$), this six-line spectrum was not observed, and a normal quadrupole splitting was evident both at 295 and 77°K.

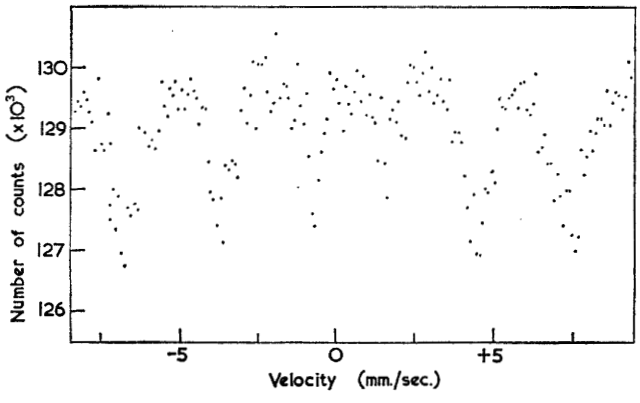

FIGURE 3 Mössbauer spectrum of $NaFeTiO_4$ at liquid-helium temperature

Replacement of Ti^{4+} by Sn^{4+} in $NaSc_{1-x}Fe_xTiO_4$ yields the isomorphous compounds $NaFeSnO_4$ and $NaScSnO_4$. ^{57}Fe parameters for $NaFeSnO_4$ and $NaFeTiO_4$ are virtually identical. In both tin compounds, the ^{119}Sn Mössbauer absorption took the form of single, broad line ($\Gamma = 1{\cdot}8$ mm./sec.), probably the result of random occupation of octahedral sites by Fe^{3+}, Sc^{3+}, and Sn^{4+}.

(2) $CaSc_{2-x}Fe_xO_4$.—$CaFe_2O_4$ [6-8] and $CaSc_2O_4$ [4] are isostructural with $NaScTiO_4$,[3] and were found to show complete isomorphous solid solution with each other. At low Fe concentration, two closely spaced e.s.r. lines near $g = 4{\cdot}3$ showed the presence both of two distinct metal-atom environments,[33] and of a large crystal-field anisotropy. The Mössbauer spectra of the series were therefore examined to discover whether they showed the same effects as observed for the $NaSc_{1-x}Fe_xTiO_4$ series, and whether Sc^{3+} and Fe^{3+} were ordered into particular sites.

In $CaFe_2O_4$ the two distinct metal-atom sites do indeed give rise to a Mössbauer spectrum having two quadrupole split absorptions, as has been reported by a number of workers.[30,31] The spectrum which we obtained, while not as well resolved as that reported by Bertaut *et al.*,[30] who used samples enriched in ^{57}Fe, gives virtually identical parameters when analysed. The scandium-substituted calcium ferrites did not show evidence for site preference by Sc^{3+}, and for $CaFeScO_4$ the spectra were best fitted by two quadrupole split absorptions with the outermost pair of lines being of somewhat lower intensity. However, in view of the assumption made in the computer fitting that the two absorptions have equal linewidths, and because the lines are not well resolved, these unequal intensities must be viewed with caution.[36] For the composition $x = 0{\cdot}20$ the best fit was obtained assuming only one quadrupole split absorption. No definite decision can be made as to the site or sites occupied by the iron remaining in $CaSc_{1{\cdot}8}Fe_{0{\cdot}2}O_4$ since the quadrupole splitting obtained matches neither of the values obtained in the parent compound. Like the two previous series discussed, a gradual increase in quadrupole splitting results as the iron content is reduced, and this is accompanied by a steady increase in linewidth. This indicates a random replacement of iron by scandium.

Decker and Kasper [8] assumed that the magnetic behaviour of $CaFe_2O_4$ would be explicable in terms of strong antiferromagnetic coupling between the iron atoms along the double chains of iron–oxygen octahedra, with only weak coupling between adjacent chains (Figure 1). This has been found to be so at sufficiently high temperatures [37,38] but neutron-diffraction studies by Bertaut *et al.*[30] and Allain and his co-workers [39] show that below 180°K (approximately), there is strong ferromagnetic coupling along each double chain, with the spins aligned up the *b* axis in the double chains of equivalent crystallographic sites of one kind, and down the *b* axis in the double chains of sites of the second crystallographic kind. For Fe^{3+} in either site the magnetic moments were found experimentally to be almost

[35] G. K. Wertheim, 'The Mössbauer Effect,' W. A. Benjamin, New York, 1963, p. 295.
[36] T. C. Gibb, R. Greatrex, and N. N. Greenwood, *J. Chem. Soc.* (*A*), 1968, 890.
[37] L. M. Corliss, J. M. Hastings, and W. Kunnann, *Phys. Rev.*, 1967, **160**, 408.
[38] H. Wanatabe, H. Yamaguchi, M. Okaski, T. Okada, and M. Fukase, *J. Phys. Soc. Japan*, 1967, **22**, 939.
[39] Y. Allain, B. Boucher, P. Imbert, and M. Perrin, *Compt. rend.*, 1966, *B***263**, 9.

identical, and the ferromagnetism of the two interpenetrating sets of double chains is thus cancelled. The net result is antiferromagnetism, with a resultant magnetic moment per formula unit of 0·025 B.M. at 4·2°K.[39] Above the Néel temperature of 180°K, the magnetic susceptibility is almost constant to 400°K, *i.e.*, in the Decker and Kasper antiferromagnetic region, but above 500°K simple paramagnetism is observed. The Weiss constant for $CaFe_2O_4$, 580°K,[39] is almost exactly twice that for the isomorphous compound $NaFeTiO_4$, 270°K, in accord with the observed linear increase in Weiss constant with Fe^{3+} concentration in the system $NaSc_{1-x}Fe_xTiO_4$.[1] The absence of a Néel point in $NaFeTiO_4$, at least above 80°K, is to be attributed to the effect of Ti atoms sufficiently interrupting the strong Fe interactions within any one chain that a fully co-operative antiferromagnetic arrangement cannot be obtained.

Yamamoto *et al.*[32] attempted to find a change in the Mössbauer spectrum of $CaFe_2O_4$ as the spin alignment changed from ferromagnetic within each chain (the low temperature situation) to spins oppositely directed within each chain (the Decker and Kasper antiferromagnetic structure). However, no change in the Mössbauer parameters from this cause could be detected, although spin-lattice relaxation, which was found to be strong in the region near the Néel temperature, may well have obscured any other effects. These workers[32] obtained a magnetic field at the Fe nucleus of 443 kgauss at 79°K, with a value extrapolated to 0°K of 485 kgauss. We find a value of 460 kgauss at liquid-nitrogen temperature. The low-temperature spectra could not be analysed in terms of two overlapping six-line spectra, which is in accord with the Fe^{3+} ions in each of the crystallographic sites having identical magnetic moments[39] in the low-temperature ferromagnetic-chain situation.

Progressive replacement of iron by scandium in $CaSc_{1-x}Fe_xO_4$ results in a disruption of $Fe\langle^{O}_{O}\rangle Fe$ interactions along the double chains of octahedra and the strong magnetic coupling is lost. $CaScFeO_4$ (magnetically equivalent to $NaFeTiO_4$) and $CaSc_{1\cdot8}Fe_{0\cdot2}O_4$ show only paramagnetic Mössbauer spectra at 77°K. However at the $x = 0{\cdot}01$ composition a strong magnetic field is again experienced by the Fe nucleus, and the spectrum at 77°K is entirely analogous to that for the $x = 0{\cdot}01$ composition in $NaSc_{1-x}Fe_xTiO_4$. At the $x = 0{\cdot}01$ concentration occupation of two kinds of site was not evident, and it must be that the small differences in ground-state energy levels which produce two distinct e.s.r. signals[33] do not affect the Mössbauer parameters sufficiently to allow detection.

(3) $Sc_{2-x}Fe_xTiO_5$.—The pseudobrookite structure[10,11] is based on metal–oxygen octahedra with all atoms in planes at $y = 0$ and $y = \frac{1}{2}$, and an a-axis repeat distance of 3·8 Å, an octahedral diagonal. Figure 4 shows a representation of the structure in terms of metal–oxygen octahedra, projected on the y–z plane. In Fe_2TiO_5 titanium is ordered into the fairly regular octahedral sites situated on mirror planes, and repeating four times in each unit cell. These octahedra lie in the V-shaped conjunctions of pairs of edge-shared octahedra containing Fe atoms, for which there are eight sites in each unit cell. The rather distorted $Fe{-}O_6$ octahedra occur in twisted chains directed along the a-axis, each roughly helical chain being connected by octahedral edge-sharing to an adjacent chain. The disposition of Fe atoms in these sites is such that individual Fe sites are connected through pairs of oxygen atoms (octahedral edges) to three other sites approximately 3·0 Å distant, one of these sites being in the same plane and two obliquely above and below in the same twisted chain. There are also connections through single oxygen atoms to the two sites 3·8 Å above and below any given metal, and to a site in the same y–z plane but in an adjacent pair of sites.

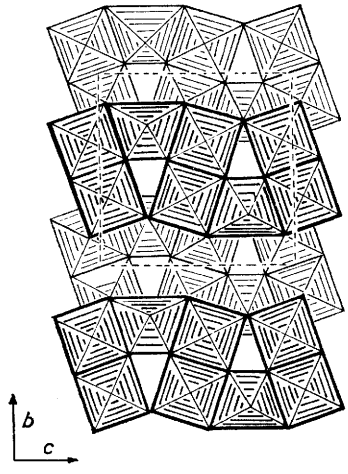

FIGURE 4 Idealised structure of Fe_2TiO_5 viewed down the 3·8Å a-axis. Metal atoms at $x = a/2$ are contained in heavily shaded octahedra, those at $x = 0$ in lightly shaded octahedra. The sites for Fe atoms occur in pairs of edge-shared octahedra, with the sites for Ti atoms lying in the V-shaped spaces between the Fe sites

In (stabilized) Sc_2TiO_5 the Sc and Ti atoms are randomized, as in $NaScTiO_4$. As the composition approaches Fe_2TiO_5 ordering occurs, and the sites are distinguishable crystallographically.[10,11] As expected for all Fe in one kind of crystallographic site, only one quadrupole-split absorption is observed for Fe_2TiO_5 (Table 2) in agreement with the results of other workers.[40] It has been suggested[40] that Fe_2TiO_5 might show antiferromagnetism at 77°K. At this temperature we could detect no change in Mössbauer parameters indicating such magnetism. However, the compound is magnetic (450 kgauss) at liquid-helium temperatures (Table 2). Spectra at intermediate temperatures were not recorded so that we do not know the point at which magnetism sets in.

Introduction of scandium into the lattice resulted in a small increase in quadrupole splitting, attributable to

[40] G. Shirane, D. E. Cox, and S. L. Ruby, *Phys. Rev.*, 1962, **125**, 1158.

greater distortion of the sites. Pure Sc_2TiO_5 does not have the pseudobrookite structure, but can be stabilized in this form by 10% of Fe_2TiO_5 or of Ti_2MgO_5 (isomorphous with Fe_2TiO_5).[9] Sc_2TiO_5 thus stabilized forms a continuous isomorphous series with either Ti_2MgO_5 or Fe_2TiO_5. Consequently we have used the composition $0{\cdot}9Sc_2TiO_5,0{\cdot}1Ti_2MgO_5$ to prepare the 1% ^{57}Fe sample. As with 1% ^{57}Fe in $NaScTiO_4$, a magnetic spectrum is obtained which is not completely resolved. The spectrum is temperature dependent, suggesting relaxation by a spin-lattice mechanism though the possibility of a spin–spin interaction is not ruled out. The magnetic field at the iron atom is estimated to be 520 kgauss.

TABLE 5

Optical absorption spectra of Fe^{3+} in $NaSc_{1-x}Fe_xO_2$ (energy in cm.$^{-1}$)

$[Fe^{3+}]$	Band position						
x	1	2	3	4	5	6	7
0·02				26,000	32,200	34,500	
0·10	10,000		20,700	25,000	30,600	34,500	
0·20	9500(br)	14,300(br)	20,800(n)	25,000(n)	29,200(n)	33,900(n)	
0·50	9300	13,900	20,800	24,700	28,600	33,300	
1·00	8800	13,300	20,600	24,400	28,600	33,300	
Assignment							
$^6A_1(^6S) \rightarrow$	$^4T_1(^4G)$	$^4T_2(^4G)$	$^4A_1,^4E(^4G)$	$^4T_2(^4D)$	$^4E(^4D)$	$^4T_1(^4P)$	$^4A_2(^4F)$
Calcd. [a]	9600 [b](br)	15,500 [b](br)	20,700 [c](n)	24,200 [c](n)	27,000 [c](n)	32,900 [d](m)	38,700 [b](n)

[a] 10 Dq = 13,300 cm.$^{-1}$, B = 900 cm.$^{-1}$, C/B = 4·0 and free ion ^6S ground state moved 6200 cm.$^{-1}$ closer to ^4G state in the bound ion to allow for covalence.[1] [b] Strong dependence on Dq. [c] No dependence on Dq. [d] Moderate dependence on Dq. br = Broad, m = medium, n = narrow.

(4) $NaFeTi_2O_8$.—This compound [14,15] has the sodium titanium bronze structure,[13] with Fe and Ti randomized into two crystallographically distinct, but structurally similar, octahedral sites. These are arranged in helical chains of octahedra repeating at 3·8 Å, the length of the octahedral diagonal and the b axis. The arrangement of the chains of octahedra in this repeat direction is the same as that in Fe_2TiO_5, but the conjunction of the chains is different, and allows for the inclusion of Na atoms in sites surrounded by eight metal–oxygen octahedra, similar to the 12-co-ordinated sites in perovskites.

As expected, the chemical-shift parameters are in accord with Fe^{3+} in an octahedral environment. The relatively low value for the quadrupole splitting indicates a smaller electric field gradient for this compound than for any of those discussed above, and both sites are equivalent so far as could be determined from the Mössbauer spectrum.

The optical spectrum of $NaFeTi_3O_8$, shown in Figure 1 of Reference 15, shows only four bands. These occur at 11,500, 16,300, 21,000, and 24,700 cm.$^{-1}$ and correspond in their positions and assignments to the first four observed bands in the spectrum of $NaSc_{1-x}Fe_xO_2$ (see Table 5).

(5) $NaSc_{1-x}Fe_xO_2$.—There exist a large number of oxides with layer structures of the general formula ABO_2,[41] where A is commonly H^+, Li^+, Na^+, Ag^+ or Cu^+, and B any of the trivalent transition-ions or a mixture of di- and tri-valent cations. Two main groups of such compounds are represented by α-$NaFeO_2$ [17] and its isomorphs, and by $CuFeO_2$ [42] and the compounds isomorphous with it. Both groups have rhombohedral structures, with, in hexagonal setting, unit-cell parameters close to a = 3·0 Å (an octahedral edge length) and c = 16 Å, the repeat distance for three layers of metal–oxygen octahedra separated by layers of monovalent ions. The α-$NaFeO_2$ structure (Figure 5) is a distortion along a cube diagonal of the sodium chloride structure type, with both Fe^{3+} and Na^+ in six-co-ordination to oxygen atoms. In the $CuFeO_2$ isomorphs, the monovalent Cu^+ or other A^+ ions are placed in linear two-fold co-ordination to oxygen, with the bonds directed along the c axis, and the correspondence with the NaCl structure is lost. Mössbauer studies have been made for $CuFeO_2$,[42] but not for α-$NaFeO_2$.

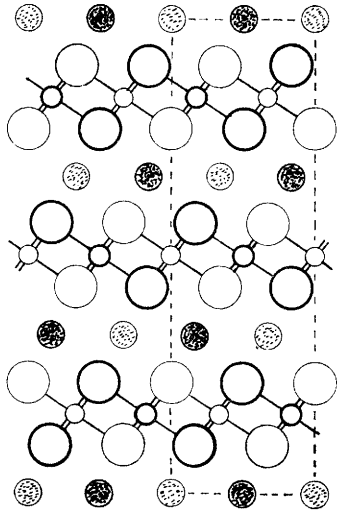

FIGURE 5 The structure of α-$NaFeO_2$, projected on the 110 plane of the hexagonal unit cell. This plane is shown in dashed outline; its dimension across the plane of projection is $a\sqrt{3}$, 5·23Å, while its dimension up the plane is the c-axis length, 16·09 Å. Small open circles Fe atoms; stippled circles Na atoms; large open circles oxygen atoms. Heavily shaded or outlined atoms lie in planes parallel to the page and separated by $a/2$, 1·51 Å, from the planes containing atoms lightly shaded

In the present work α-$NaFeO_2$ [17] was found to form an

[41] R. W. G. Wyckoff, 'Crystal Structures,' Interscience, New York, 1964, vol. 2, p. 292.

[42] A. H. Muir and H. Weidersich, *J. Phys. Chem. Solids*, 1967, **28**, 65.

isomorphous solid-solution series with $NaScO_2$.[16] The octahedral co-ordination of Fe^{3+} (or Sc^{3+}) in flat sheets of edge-shared metal–oxygen octahedra lying normal to the 16 Å *c* axis is shown in Figure 5. The 3+ metal

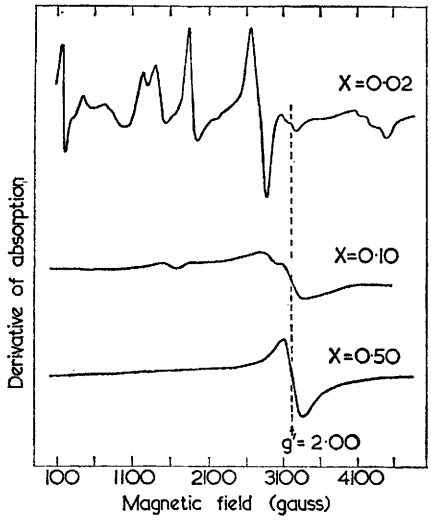

FIGURE 6 E.s.r. spectra of Fe^{3+} in powder samples of $NaSc_{1-x}Fe_xO_2$

sites are all equivalent, and all six bond-lengths are equal. The sodium atoms in the layers separating the metal–oxygen sheets, also six-co-ordinated, have equal separations from three oxygen atoms in each of the adjacent oxygen layers, and lie at the triangular faces of two metal–oxygen octahedra, one in each adjacent sheet. The metal atoms at each octahedron centre are thus in the field of six oxygen atoms in an octahedron

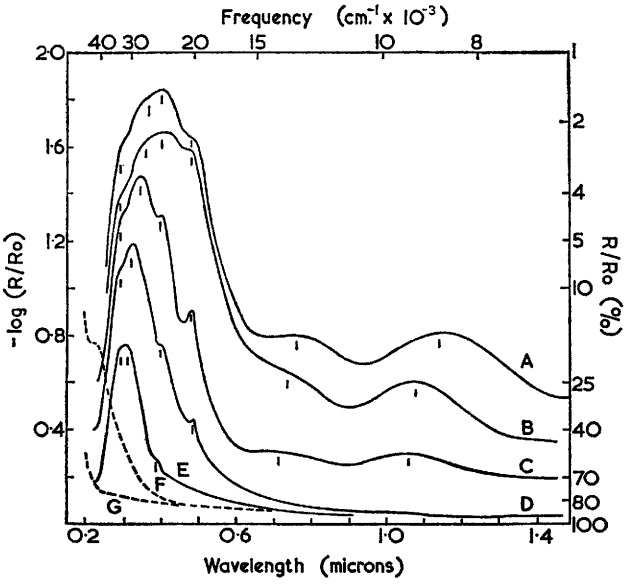

FIGURE 7 Optical absorption spectra of Fe^{3+} in $NaSc_{1-x}Fe_xO_2$. Curve A, $x = 1{\cdot}00$; B, $x = 0{\cdot}50$; C, $x = 0{\cdot}20$; D, $x = 0{\cdot}10$; E, $x = 0{\cdot}02$. Band centres are shown by a single dash. Curve F shows the absorption of the host lattice reference compound $NaScO_2$, *vs.* MgO as reference. Curve G shows the cancellation obtained for $NaScO_2$ as both sample and reference

oblique to the *c*-axis and are also affected by sodium ions disposed obliquely with respect to the *c*-axis. A strongly anisotropic crystal-field is thus to be expected at each metal atom site. A marked effect is indeed observed in the e.s.r. spectra of low concentrations of Fe^{3+} in $NaSc_{1-x}Fe_xO_2$ (Figure 6) and the optical spectra (Figure 7 and Table 5) appear to show all six of the lower-energy electronic transitions possible when an initially cubic field about the $3d^5$ Fe^{3+} ion is distorted. As in $NaSc_{1-x}Fe_xTiO_4$,[1] the relative intensities of the transitions vary strongly with Fe^{3+} concentration, but the $^6A_1(^6S) \longrightarrow {}^4E(^4D)$ transition does not in the present case completely disappear as the Fe^{3+} concentration increases. Assignments based on those previously calculated are given

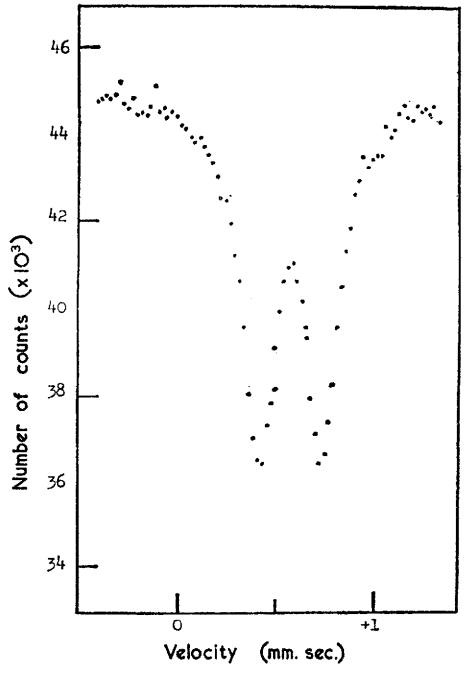

FIGURE 8 Mössbauer spectrum of α-$NaFeO_2$ at 77°K

in Table 5 and the overall agreement strongly supports their correctness.

The magnetic susceptibilities of $NaSc_{1-x}Fe_xO_2$ as a function of concentration (Table 4) show Fe^{3+} to be in the high-spin state, although with magnetic moment somewhat less than the 'spin-only' value. A Curie–Weiss law is obeyed at sufficiently high temperatures but it is striking that θ decreases to negative values as the fraction of Fe^{3+} increases, in complete contrast to the behaviour of the other systems listed in Table 5. This would appear to indicate a form of ferromagnetic interaction, but α-$NaFeO_2$ does not show a magnetic Mössbauer spectrum at either 295 or 77°K (Figure 8). However, it may become magnetic at liquid-helium temperatures. $CuFeO_2$, which has the same arrangements of Fe^{3+} sites but not of A^+ ions was found to exhibit a magnetic transition at 20°K.

Mössbauer data for the $NaSc_{1-x}Fe_xO_2$ series (Table 2) show little change in the parameters for α-$NaFeO_2$

(Figure 8) as scandium is introduced, apart from a small but significant increase in quadrupole splitting, and a broadening of the spectrum at $NaSc_{0.95}Fe_{0.05}O_2$. However, at the very low Fe^{3+} concentration $x = 0.005$, with iron enriched to 91% in ^{57}Fe, a partial magnetic spectrum was obtained at 77°K. The outer four lines of this spectrum were less well developed than in the other dilute samples we have examined, and are barely discernible in the spectrum at 295°K. At 340°K, the wings are completely collapsed into the central peak. While the magnetic field is higher than for the other samples, spin relaxation is evidently also more effective. The magnetic Mössbauer spectrum is removed either by increasing temperature at low Fe^{3+} concentration (spin-lattice relaxation) or by increasing the Fe^{3+} concentration. In the latter case some form of Fe^{3+}–Fe^{3+} interaction is indicated but as it is operative when Fe^{3+} ions are on the average approximately 4 sites apart in the planar array of available octahedral position (Figure 5) it is not possible at present to decide whether dipolar interaction or superexchange is responsible for the relaxation process.

The e.s.r. behaviour of low concentrations of Fe^{3+} in $NaSc_{1-x}Fe_xO_2$ was most unusual (Figure 6 and Table 3). Instead of a single strong line at $g = 4.3$ for low concentrations of Fe^{3+}, a series of at least 12 resonance lines was obtained, extending from $g' = 32$ to $g' = 1.45$. It is evident that a complicated interaction of the five 3*d*-electrons either with each other or with the host lattice is occurring, an effect which is probably related to the unusual Curie–Weiss behaviour for higher Fe^{3+} concentrations. Fe^{3+}–Fe^{3+} interaction appears unlikely as the cause of the $x = 0.02$ spectrum, firstly because it would involve Fe^{3+} ions approximately 7 sites apart, and secondly because such interaction at higher concentrations removes this ' isolated ion ' spectrum and produces a single, strong absorption at $g' = 2.00$ (Figure 6).

The $x = 0.02$ spectrum is consistent with a large crystal-field splitting of the ground state ^6S term of the Fe^{3+} ion, provided that transitions $m_s = \pm 1$ are allowed among all three Kramers doublets $S = \pm 5/2, \pm 3/2, \pm \frac{1}{2}$. Somewhat similar spectra have been observed for Fe^{3+} in octahedral sites in single crystal topaz,[43] and the present powder-spectrum could have arisen from the random superposition of spectra appropriate to particular orientations of the crystalline axes with respect to the external magnetic field. Single-crystal data are evidently required before this system can be fully understood and work on the growth of $NaScO_2$ single crystals is in progress.

(6) $Cs_xSc_{x-y}Fe_yTi_{2-x}O_4$.—The compounds in this series are of general formula $M^+_xA^{3+}_xTi_{2-x}O_4$ $(0.60 < x < 0.80)$ are typified by the composition $Rb_{0.75}Mn_{0.75}Ti_{1.25}O_4$ and for which a single-crystal determination has recently been reported.[21] M is Rb or Cs and A may be any of Al, Sc, Ti, Mn, or Fe. The series also contains the members $M^+_xB^{2+}_{x/2}Ti_{2-x/2}O_4$, where B is any of Mg, Fe, Co, Ni, Cu, or Zn. Preliminary experiments have shown that solid solutions are formed between any two members, and as well as the results reported here for the iron-containing isomorphs a number of other measurements will be reported elsewhere. The layer structure of this isomorphous series of compounds is non-centrosymmetric, and is illustrated in Figure 9. Cs atoms lie in planes normal to the 17 Å *b*-axis, and separate puckered sheets of edge-shared metal–oxygen octahedra. All metal atom sites are equivalent, and Sc, Fe, and Ti are therefore randomly distributed in them. The sheets of octahedra are identical with those in lepidocrocite, FeO(OH); the correspondence between sheets is however altered to accommodate Cs or Rb in eightfold co-ordination to oxygen rather than H atoms in two-fold co-ordination. The Cs atom positions are only partially occupied, and the ratio of 3+ to 4+ ions in the (fully occupied) octahedral sites is correspondingly adjusted to maintain charge balance.

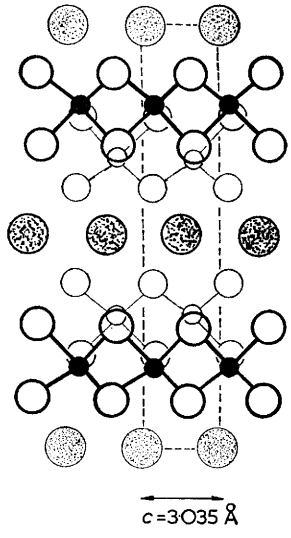

FIGURE 9 The noncentrosymmetric structure of $Cs_xFe_xTi_{2-x}O_4$, projected down the 3·805 Å *a*-axis. The polar axis, *c*, lies across the plane of projection. Small circles Fe or Ti atoms, larger open circles oxygen atoms, large stippled circles Cs atoms. Heavily marked atoms are in planes parallel to the page and separated by *a*/2 from those containing lightly marked atoms

Metal atom sites are not symmetrically placed with respect to Cs atoms and adjacent octahedra, and the consequent considerable lowering of crystal field symmetry from cubic produces at low Fe^{3+} concentrations an e.s.r. absorption which is strongly anisotropic, $g' = 4.34$ (Figure 10). The weak signal at $g' = 2.05$ for $Cs_{0.67}Sc_{0.65}Fe_{0.02}Ti_{1.33}O_4$ presumably disappears at even lower Fe^{3+} concentrations, but at increased concentration increases to a strong broad absorption at $g' = 2.06$ and the $g' = 4.34$ line is completely removed (Figure 10). The displacement of the exchange-coupled e.s.r. signal from $g' = 2.00$ in $NaSc_{1-x}Fe_xTiO_4$ and $NaSc_{1-x}Fe_xO_2$ to $g' = 2.06$ in $Cs_{0.67}Fe_{0.67}Ti_{1.33}O_4$ is

[43] J. R. Thyer, S. M. Quick, and F. Holuj, *Canad. J. Phys.*, 1967, **45**, 3597; F. Holuj and S. M. Quick, *Canad. J. Phys.*, 1968, **45**, 1087.

presumably due to the crystal field within the noncentrosymmetric structure which provides some spin alignment with respect to the polar *c*-axis even when the spins are exchange-coupled.

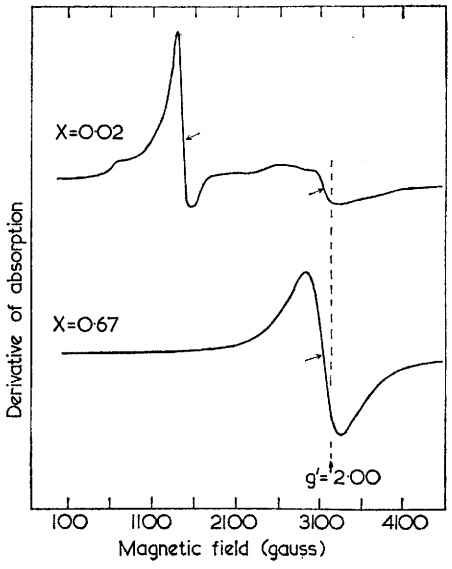

FIGURE 10 E.s.r. spectra of Fe^{3+} in powder samples of $Cs_{0\cdot67}Sc_{0\cdot65}Fe_{0\cdot02}Ti_{1\cdot33}O_4$ ($x = 0\cdot02$) and $Cs_{0\cdot67}Fe_{0\cdot67}Ti_{1\cdot33}O_4$ ($x = 0\cdot67$). The arrows mark the absorption signal centres for which g' values are given in Table 3

As with the other systems studied, magnetic susceptibility measurements (Table 4) show the Fe^{3+} ions to be in the high-spin state. However, a high Weiss temperature, 133°K, and an effective magnetic moment of 5·39 B.M. per atom rather than 5·92 for the spin free case, confirms the presence of considerable antiferromagnetic coupling. The electronic absorption spectrum (Table 6) shows the usual change in relative band intensities (Figure 14) with the transition $^6A_1(^6S) \longrightarrow {}^4T_2(^4G)$ being absent at 300°K, as was also the case for $NaSc_{1-x}Fe_xTiO_4$.[1]

TABLE 6

Optical absorption spectra of Fe^{3+} in $Cs_{0\cdot67}Sc_{0\cdot67-y}Fe_yTi_{1\cdot33}O_4$ (energy in $cm.^{-1}$)

$[Fe^{3+}]$	Band position [a]				
y	1	3	4	5	6
0·02		20,800	24,100		30,600
0·05		20,700	24,100		30,100
0·10	11,800	20,600	23,900	27,800	29,700
0.20	11,800	20,600	23,800	26,700	
0·67	11,700	20,500	23,500	26,000	
Assignment					
$^6A_1(^6S) \rightarrow$	$^4T_1(^4G)$	$^4A_1{}^4E(^4G)$	$^4T_2(^4D)$	$^4E(^4D)$	$^4T_1(^4P)$
Calcd.	9,600	20,700	24,200	27,000	32,900

[a] The transition $^6A_1(^6S) \rightarrow {}^4T_2(^4G)$ was not observed.

The effects observed in the e.s.r. spectrum are paralleled by the Mössbauer data (Table 2). Due to the attenuation of the γ-rays by the heavy caesium atoms, poor counting statistics were observed for the $x = 0\cdot01$ spectra, and the parameters quoted are approximate. However, a partially resolved six-line magnetic spectrum was observable at this concentration, replaced at higher concentrations by a quadrupole split absorption. The chemical shift and quadrupole splitting parameters certainly bear out the noncentrosymmetric, octahedral arrangement about the iron atoms.

(7) β-$NaAl_{1-x}Fe_xO_2$.—β-$NaAlO_2$[18] and β-$NaFeO_2$[19] are isomorphous with β-$LiGaO_2$,[44] and atomic co-ordinates have been determined for the second two.[19,44] The structure is illustrated for β-$NaFeO_2$ in Figure 12. Each of Na, Fe, and O are tetrahedrally co-ordinated in an orthorhombic distortion of the wurtzite (ZnS) structure type, which can be considered as an infinite three-dimensional array of tetrahedra having only corners in common, and with all tetrahedra having a vertex directed in the same sense along the *c*-axis. This structure is, like β-$LiGaO_2$ (and ZnS), noncentrosymmetric and in it Fe and Na atoms are ordered out in pairs. Oxygen atoms define the corners of the tetrahedra, and each Fe atom at a tetrahedron centre is linked through single oxygen atoms to four further Fe atoms. Only the conjunction of the $Fe{-}O_4$ tetrahedra

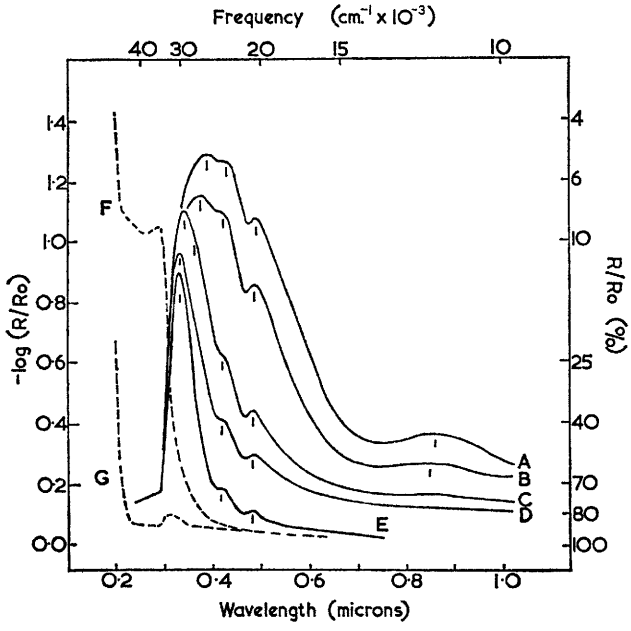

FIGURE 11 Optical absorption spectra of Fe^{3+} in $Cs_{0\cdot67}Sc_{0\cdot67-y}Fe_yTi_{1\cdot33}O_4$. Curve A, $y = 0\cdot67$; B, 0·20; C, 0·10; D, 0·05; E, 0·02. Curve F shows the absorption of the titanate host lattic $Cs_{0\cdot67}Sc_{0\cdot67}Ti_{1\cdot33}O_4$ used as reference sample for curves A to E, with MgO as its reference. Curve G shows the cancellation obtained when the host lattice was used as sample and reference. The residual absorption near 0·3 microns was not significantly altered in intensity either by use of a variety of particle sizes for the sample, or by small alterations in the positions of the sample and reference in the spectrophotometer reflectance housing

is shown in Figure 12; the $Na{-}O_4$ tetrahedra lie in a second entirely similar array which interpenetrates the first. In β-$NaAl_{1-x}Fe_xO_2$ solid solutions, Fe and Al, which occupy equivalent crystallographic sites in

[44] M. Marezio, *Acta Cryst.*, 1965, **18**, 481.

β-$NaAlO_2$ and β-$NaFeO_2$, will be randomly distributed in the one kind of crystallographic site which builds up the array shown in Figure 16. The Mössbauer data for the series (Table 2 and Figure 18) certainly confirms that the iron is in a tetrahedral rather than an octahedral environment. Unlike α-$NaFeO_2$, β-$NaFeO_2$ has a magnetic Mössbauer spectrum at room temperature, with a small quadrupole splitting being also evident. Wanatabe and Fukase [20] have reported a slight ferromagnetism which coexists with antiferromagnetism below the Néel point of 450°K, and Bertaut *et al.*[45] have shown by neutron diffraction measurements that there is almost complete antiferromagnetic ordering at 300°K, with an opposite ordering of spins between any given Fe atom and the Fe atoms to which it is joined by

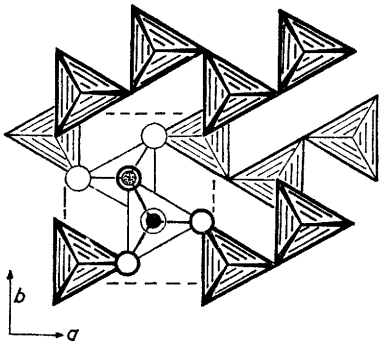

FIGURE 12 Representation of the Fe–O_4 tetrahedra in β-$NaFeO_2$, projected down the *c*-axis. Oxygen atoms lie at the apices and Fe atoms at the centres of the tetrahedra, which occur in pairs in the *x*–*y* plane, and are joined in staggered strings in the *c*-axis direction. The tetrahedral Fe–O distances are 1·79 Å directed up the *c*-axis, and variously 1·81, 2·03, and 2·18 Å for the bonds to oxygen atoms forming the bases of the tetrahedra. Sodium atoms are omitted from this projection, but form a similar set of Na–O_4 tetrahedra interpenetrating those shown and using the same oxygen atoms as apices.

tetrahedral corner sharing. Our own magnetic-susceptibility measurements showed that feeble ferromagnetism persists in β-$NaAl_{1-x}Fe_xO_2$ for $x \geqslant 0{\cdot}5$, and the Mössbauer spectra (Figure 13) show that the magnetic field at the Fe nuclei (due to the antiferromagnetic spin alignment) is retained for at least 10%, and probably considerably more, of Al substituting for Fe. Between $x = 0{\cdot}5$ and $x = 0{\cdot}1$, the magnetic field is lost, but it reappears again as the isolated Fe^{3+} situation is approached.

The e.s.r. spectrum of Fe^{3+} at low concentration in β-$NaAl_{1-x}Fe_xO_2$ is shown in Figure 14. There is a strong, very broad resonance centred at $g' = 2{\cdot}10$, and two sharper resonances at $g' = 4{\cdot}30$ and $g' = 3{\cdot}75$. These last are consistent with an anisotropic *g* tensor and a strong rhombic crystal field, while the strong $g' = 2{\cdot}10$ resonance indicates that there may be some degree of Fe^{3+}–Fe^{3+} coupling by way of the lattice even at $x = 0{\cdot}02$. At higher concentrations the resonance near $g' = 4$ disappears and that at $g' = 2$ is narrowed and moved to $g' = 2{\cdot}020 \pm 0{\cdot}005$ for $x = 0{\cdot}30$.

The optical absorption spectrum of β-$NaAl_{1-x}Fe_xO_2$ was poorly resolved at $x = 0{\cdot}02$ and at high concentrations the bands above 15,000 $cm.^{-1}$ were too intense to be resolved. However at $x = 0{\cdot}10$ seven distinct absorptions were evident (Table 7). The band positions were similar to those for Fe^{3+} in $NaSc_{1-x}Fe_xO_2$, with the additional feature of a band corresponding to the $^6A_1(^6S) \longrightarrow {}^4T(^4F)$ transition, and comparable intensities.

A probable assignment for the spectrum of the tetrahedrally co-ordinated Fe^{3+} is given in Table 7 and, as expected for a d^5 system, the band sequence corresponds

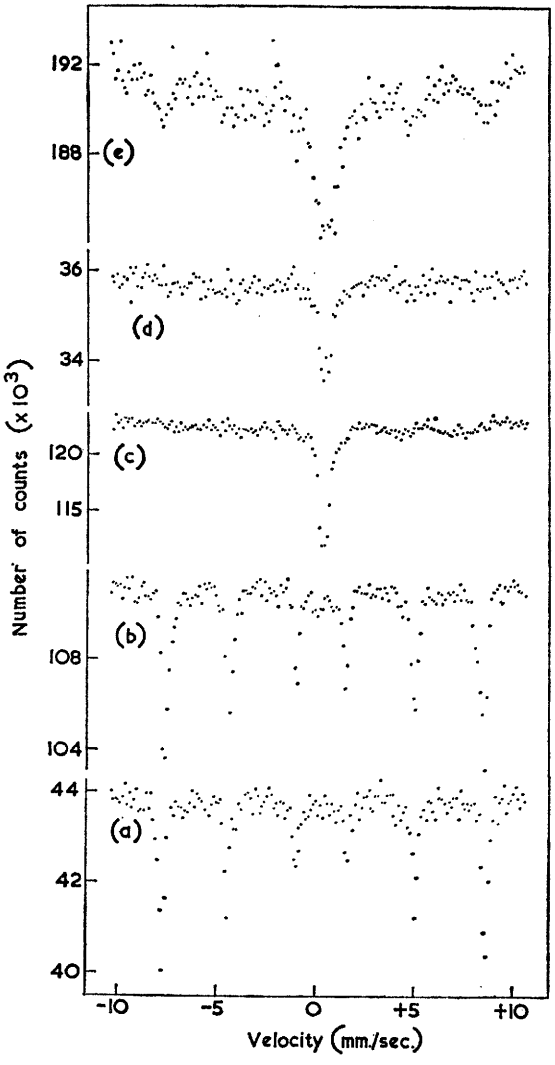

FIGURE 13 Mössbauer spectra of β-$NaAl_{1-x}Fe_xO_2$ at 295°K; (a) $x = 1$, (b) $x = 0{\cdot}90$, (c) $x = 0{\cdot}50$, (d) $x = 0{\cdot}10$, and (e) $x = 0{\cdot}01$

to that assigned for octahedrally co-ordinated Fe^{3+} (Table 5).

From the e.s.r. and Mössbauer spectra for Fe^{3+} in β-$NaAl_{1-x}Fe_xO_2$ it is evident that strong coupling forces are operating in this lattice, and that single-crystal data should be most informative. The growth of single

[45] F. Bertaut, A. Delapalme, and G. Bassi, *Compt. rend.*, 1963, p. 421.

TABLE 7

Optical absorption of tetrahedrally co-ordinated Fe^{3+} in β-$NaAl_{1-x}Fe_xO_2$ (energy in $cm.^{-1}$)

[Fe+]	Band position						
x	1	2	3	4	5	6	7
0·10	11,600	15,600	19,000	22,700	26,000	33,900	41,700
0·30	9,800	16,600	20,000	23,800	u	u	u
0·90	9,800	16,600	20,400	u	u	u	u
Possible assignment							
$^6A_1(^6S) \rightarrow$	$^4T_1$-(^4G)	$^4T_2$-(^4G)	$^4A_1$, $^4E(^4G)$	$^4T_2$-(^4D)	$^4E(^4D)$	$^4T_1(^4P)$	$^4A_2(^4F)$
Calcd.	9,600	15,500	20,900	24,200	27,000	32,900	38,700

u = Strong but unresolved.

crystals of compositions in this system is at present being attempted.

(**8**) $Cs_xSc_{x-y}Fe_yTi_{4-x}O_8$.—The hollandite structure [22] was shown by Bayer and Hoffman [23] to be adopted by a number of ternary transition-metal titanates of theoretical end member composition $ABTi_3O_8$ where A is K^+, Rb^+, or Cs^+, and B is a trivalent metal ion or represents an equiatomic mixture of a divalent metal ion and tetravalent titanium. Composition limits were not determined, but in the present work we have found that a single-phase hollandite structure exists at each of the compositions $Cs_{0·63}Sc_{0·63}Ti_{3·37}O_8$ and $Cs_{0·70}Fe_{0·70}Ti_{3·30}O_8$, and that these two hollandites form an isomorphous solid solution series.

Like the $NaScTiO_4$ (calcium ferrite) structure (Figure 1) the hollandite structure is built up of double blocks of edge-shared octahedra, themselves repeating by edge-sharing along the 3 Å axis, the octahedral edge length.

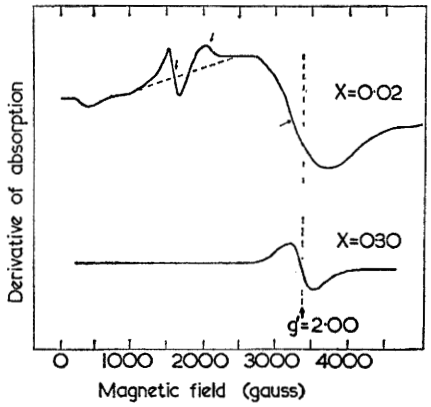

FIGURE 14 E.s.r. spectra of Fe^{3+} in β-$NaAl_{0·98}Fe_{0·02}O_2$ and β-$NaAl_{0·70}Fe_{0·30}O_2$. The arrows mark the absorption signal centres for which g' values are given in Table 3, and the dashed line in the $x = 0·02$ curve indicates the shape of the broad $g' = 2·10$ absorption derivative on which are superimposed the two signals at $g' = 3·75$ and $g' = 4·30$.

The chains of double blocks are corner-connected to form the tetragonal array shown in Figure 15. All the octahedral sites are equivalent, and B^{3+} and Ti^{4+} ions will therefore be randomized in them. The open tunnels between the chains provide sites 3 Å apart for the alkali-metal ions, and since these are large, less than 75% of the sites are in general occupied. The fully occupied three-dimensional framework of metal–oxygen octahedra defines the structure, however, and lattice parameters are insensitive to the fractional occupancy shown by the alkali (or alkaline-earth) ions.

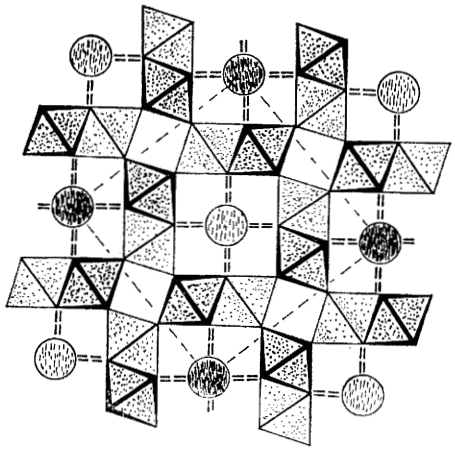

FIGURE 15 Projection down the 3 Å c-axis of the tetragonal hollandite structure of $Cs_{0·7}Fe_{0·7}Ti_{3·3}O_8$. Octahedra with heavy markings contain Fe or Ti at $x = c/2$ in planes parallel to the page and separated by $c/2$ from those in the lightly marked octahedra. Cs atoms are shown by circles; those with heavy strippling lie in planes at $x = c/2$ and those lightly stippled lie at $x = 0$. Only 0·7 of the Cs atom sites are occupied in the real structure. The unit cell is shown by lightly dashed lines. Heavy dashed lines show the nearest neighbour connections for each Cs atom, namely to oxygen atoms in planes $c/2$ above and below the plane containing the Cs atom

As for $NaScTiO_4$, each octahedral metal-atom site has octahedral sites both directly and obliquely above and below it in a given double chain. The faces of the octahedra are adjacent to alkali-ion sites however, and a strong rhombic field is again expected at each octahedral site.

Mössbauer data for $Cs_{0·70}Fe_{0·70}Ti_{3·30}O_8$ and $Cs_{0·63}Sc_{0·43}Fe_{0·20}Ti_{3·37}O_8$ show a single quadrupole split absorption in Table 2, in accord with Fe^{3+} randomized into one kind of site. At low concentrations, using ^{57}Fe in the composition $Cs_{0·63}Sc_{0·62}Fe_{0·01}Ti_{3·37}O_4$, we again observed a magnetic spectrum at 77°K (Table 2) and at a comparable composition a single strong symmetrical e.s.r. signal centred at $g' = 4·45$ was also obtained (Table 3).

The optical spectra of Fe^{3+} in the hollandite host lattice (Table 8) were similar to those of the other com-

TABLE 8

Optical absorption spectra of Fe^{3+} in $Cs_xSc_{x-y}Fe_yTi_{4-x}O_8$ (energy in $cm.^{-1}$)

	Band position				
[Fe^{3+}]	1	2	3	4	5
$x = 0·63$, $y = 0·05$	9,500	14,100	20,400	—	26,000
$x = 0·63$, $y = 0·20$	9,500	13,900	20,400	24,400	25,300
$x = 0·70$, $y = 0·70$	9,300	13,300	20,400	23,500	25,300
Assignment					
$^6A_1(^6S) \rightarrow$	$^4T_1(^4G)$	$^4T_2(^4G)$	$^4A_1$, $^4E(^4G)$	$^4T_2(^4D)$	$^4E(^4D)$
Calcd.	9600	15,500	20,700	24,200	27,000

pounds studied, except that the $^6A_1(^6S) \longrightarrow {}^4T_1(^4P)$ transition was not observed.

(9) $LiFeTiO_4$.—This compound has the spinel structure, and *X*-ray data [24] indicate that Fe^{3+} is equally distributed over tetrahedral and octahedral sites, with a consequent overall atom distribution $(Li_{\frac{1}{2}}Fe_{\frac{1}{2}})[Li_{\frac{1}{2}}Fe_{\frac{1}{2}}Ti]O_4$, the square braces representing octahedral sites. The magnetic susceptibility of $LiFeTiO_4$ at room temperature was found in the present work to be 10 to 20 times higher than attributable to simple paramagnetism, indicating a Curie temperature not far below 295°K. The Mössbauer spectrum consists of a broad doublet at 295°K, but at 77°K the sample showed a full magnetic spectrum (Figure 16). This spectrum was best analysed for two overlapping six-line patterns of equal intensity, thus indicating equal distribution of Fe^{3+} in two kinds of sites, in accord with the *X*-ray data.

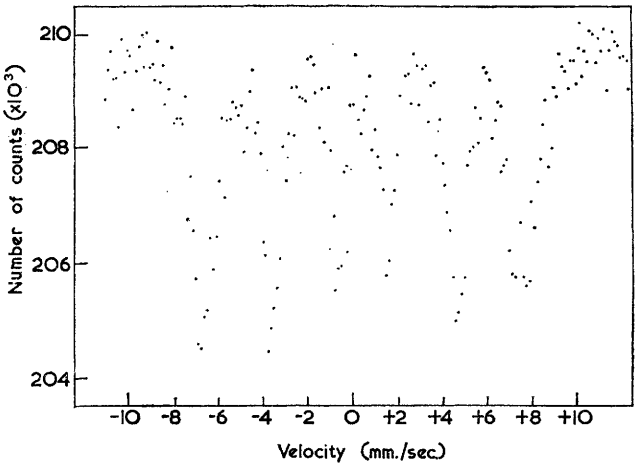

FIGURE 16 Mössbauer spectrum of $LiFeTiO_4$ at 77°K.

Attempts to alter the ordering in $LiFeTiO_4$, or find an order-disorder transition as in $Li_{0.5}Fe_{2.5}O_4$ [46,47] were unsuccessful. The *X*-ray diffraction intensities and the Mössbauer spectra were unchanged for samples prepared or annealed at temperatures in the range 300—1000°.

(10) $CsFeSi_2O_6$.—This compound is isomorphous with pollucite ($CsAlSi_2O_6$) [25] and has previously been prepared by hydrothermal methods.[26] It was found in the present work to form readily in the crystalline state by the reaction at 800° of $CsNO_3$ with Fe_2O_3 and amorphous precipitated silica, although the aluminium pollucite could not be crystallized under similar conditions. Natural and hydrothermally prepared pollucites always contain some water,[25,26] substituted for Cs in the large cage positions formed by the network of interconnecting rings of four and six metal–oxygen tetrahedra. For $CsFeSi_2O_6$(aq.) the unit-cell parameter was found by Kume and Koizumi [26] to be 13·816 ± 0·002 Å; the anhydrous compound prepared in the present work had $a_0 = 13{\cdot}81 \pm 0{\cdot}01$. The hydrothermally prepared compound was reported to be paramagnetic,[26] and in the present work we have found the anhydrous compound also to be paramagnetic in the range 120—370°K. The Weiss constant was 72 ± 4°K, a normal value, but the Curie constant was much lower than normal, with a resulting μ_{eff} value of 4·26 B.M. (Table 4). This value is not as low as for low-spin Fe^{3+}, 2·3 B.M., but does indicate a strong co-operative coupling between Fe^{3+} pairs or clusters.

In the Mössbauer spectrum (Table 2) both the chemical shift and the quadrupole splitting lie in the ranges observed for tetrahedral Fe^{3+},[48] and the spectrum is consistent with one kind of Fe^{3+} site. In pollucite Al and Si are randomized into the 48 crystallographically equivalent sites available in each unit cell,[25] and Fe and Si are presumably similarly randomized in the isomorphous $CsFeSi_2O_6$, with one-third of sites occupied by Fe^{3+}. As we have found in β-$NaAl_{1-x}Fe_xO_2$, tetrahedral interactions can be very strong. In $CsFeSi_2O_6$ the interaction is apparently antiferromagnetic rather than ferromagnetic, and studies to determine its nature would be worthwhile.

DISCUSSION

The main conclusion to be drawn from the results of the present work is that the same rhombic crystal field environment which splits the ground-state levels of an isolated $3d^5$ Fe^{3+} ion in a crystalline host lattice and produces a strong e.s.r. signal at $g' = 4{\cdot}3$, also produces a six-line magnetic Mössbauer spectrum. As the Fe^{3+} concentration in the lattice is increased, both the e.s.r. signal and the Mössbauer spectrum are altered, the first to an absorption at $g' = 2{\cdot}00$ and the second to a normal paramagnetic quadrupole split absorption. The changes in the Mössbauer spectra do not exactly follow those of the e.s.r. absorptions, in that the Mössbauer spectra generally change at lower Fe^{3+} concentrations, and are also altered at temperatures at which the $g' = 4{\cdot}3$ e.s.r. signals persist. We conclude that the e.s.r. and Mössbauer 'isolated-ion' effects arise from similar causes, but that they are not entirely interdependent.

The work of Castner, Newell, Holton, and Slichter [49] on Fe^{3+} in glasses, and of Wickman, Klein, and Shirley [2] on Fe^{3+} in the compound ferrichrome A, shows that $g' = 4{\cdot}3$ e.s.r. signals are characteristic of Fe^{3+} in a rhombic crystal field for which the crystal field contributions to the spin Hamiltonian are larger than the Zeeman term $g_0\beta H{\cdot}S$. Castner *et al.*[49] treated a spin Hamilton of the form:

$$\mathscr{H} = g_0\beta HS_{z'} + DS_z^2 + E(S_x^2 - S_y^2)$$

where D and E are constants, S_x, S_y and S_z are components of spin along three mutually perpendicular

[46] J. P. Remeika and R. L. Comstock, *J. Appl. Phys.*, 1964, **35**, 3320.

[47] A. J. C. Wilson, ed. for I.U.P.A.C., 'Structure Reports,' N.V.A. Oosthdek's Uitgevers Mij, Utrecht, Netherlands, 1950, **13**, 245.

[48] G. M. Bancroft and A. G. Maddock, *Geochim. Cosmochim. Acta*, 1967, **31**, 2219.

[49] T. Castner, G. S. Newell, W. C. Holton, and C. P. Slichter, *J. Chem. Phys.*, 1960, **32**, 668.

crystal field axes, z' is the axis of the applied magnetic field H, and g_0 has the free spin g value of 2, *i.e.*, the value expected when $D = E = 0$. The terms in D and E express the preference of the spin to line up along particular crystalline directions, and for strong axial or rhombic fields D and E have been found [1,49–55] to lie in the range 0·5—10 cm.$^{-1}$, as compared with 0·3 cm.$^{-1}$ for X-band microwave frequencies. On the assumption that such values apply, and taking initially $H = 0$, the Hamiltonian can be treated for the terms in D and E and the effects of the applied field H then included as a perturbation. For the special case $E = 0$ there is axial field symmetry and for z' perpendicular to z, a strong anisotropic $g' = 6$ line results. As the field is rotated until z' is parallel to z, the g' value changes continuously until $g' = 2$. Such spectra have been observed for Fe^{3+} in haemoglobin ($D \sim 10$ cm.$^{-1}$),[50,51] some glasses, and for cubic crystals of $KTaO_3$,[52] ZnSe [53] and $SrTiO_3$ [54] ($D = 2{\cdot}85$ cm.$^{-1}$) containing Fe^{3+} in substitutional sites.

When $D \ll E$ a second special case arises,[49] in which the three equally-spaced Kramers doublets into which the $^6S_0$ ground state is split by the rhombic field are separated in energy by an amount, $2\sqrt{7}E$, which is large compared with the microwave quantum of energy. The splitting of the middle doublet, $S = \pm\frac{1}{2}$, by the applied magnetic field is then characterized by $g' = 30/7$, *i.e.*, 4·286, independent of the orientation of H with respect to the crystal axes. The upper and lower Kramers doublets give rise to anisotropic g' values for which the principal values are $g' \simeq 10$, 0·9, and 0·6. Since these values are obtained only for certain field orientations, the e.s.r. signals are therefore much weaker for powder specimens than is the isotropic $g' = 4{\cdot}3$ signal. The more general Hamiltonian treated by Wickman, Klein, and Shirley,[2] using a transposition of the axes chosen by Castner *et al.*[49] leads to similar results as to the g' values to be expected. In ferrichrome A the weak $g' \simeq 10$ and $g' \simeq 1$ absorptions could be observed at low temperatures, and in glasses Castner *et al.* observed a weak $g' \simeq 10$ line. In the present work we also observe a small signal near $g' = 10$ for Fe^{3+} in the $Cs_{0{\cdot}70}Sc_{0{\cdot}70}Ti_{1{\cdot}30}O_4$ host lattice, in addition to the very strong $g' = 4{\cdot}3$ line (Figure 10).

The e.s.r. results, summarized in Table 3, show that rhombic crystal fields dominate the spectra of low concentrations of Fe^{3+} in the host lattices $NaScTiO_4$ (orthorhombic), $Cs_{0{\cdot}67}Sc_{0{\cdot}67}Ti_{1{\cdot}33}O_4$ (orthorhombic) and $Cs_{0{\cdot}63}Sc_{0{\cdot}63}Ti_{3{\cdot}37}O_8$ (tetragonal), but that in $NaScO_2$ (rhombohedral) a more complex spectrum occurs. This spectrum appears to be derived from transitions among all three pairs of Kramer's doublets rather than within each pair as in the case for strong rhombic fields,[2,49] and may be similar to that of Fe^{3+} in topaz.[43] In β-$NaAlO_2$ (orthorhombic) the $g' = 4{\cdot}30$ and $g' = 3{\cdot}75$ lines are consistent with a strong rhombic field. However the very strong, broad $g' = 2{\cdot}10$ absorption must arise from a different cause, possibly associated with the interactions which give rise to room temperature antiferromagnetism and weak ferromagnetism in β-$NaFeO_2$ [45] and which we found to persist down to $x = 0{\cdot}5$ in β-$NaAl_{1-x}Fe_xO_2$.

From the Mössbauer results we must also conclude that the same rhombic crystal fields that cause the spin to attempt to align parallel to some crystalline direction, and which result in $g' = 4{\cdot}3$ e.s.r. signals, can also hold the spin sufficiently directed that so far as the ^{57}Fe nucleus is concerned, the situation is akin to ferromagnetic or antiferromagnetic alignment, with a resultant magnetic field gradient at the iron nucleus. The ^{57}Fe nuclear spin state levels are thus split, and the characteristic six-line magnetic spectrum results. This effect is strong at low temperatures, but spin-lattice relaxation may remove the alignment at temperatures in the region 80–300°K and it is also removed as the Fe^{3+} concentration increases. The greater sensitivity of the Mössbauer effect to changes of temperature or Fe^{3+} concentration suggests different relaxation times or processes for Mössbauer and e.s.r. effects and, in particular, that the magnetic Mössbauer spectra are a pure spin-alignment effect, while the $g' = 4{\cdot}3$ e.s.r. signals are the result of ground state splittings which occur even when the spins are not strictly aligned with respect to some crystalline direction.

Magnetic hyperfine structure in the Mössbauer spectrum of Fe^{3+} in low concentrations in an oxide host lattice has also been observed by Wertheim and Remeika.[56] These authors studied Al_2O_3 single crystals in which 0·08 atom % of Al was replaced by ^{57}Fe, and were able to show that the Fe^{3+} spins were aligned with respect to the crystalline axes. Similar spectra for ^{57}Fe in V_2O_3 have been attributed to antiferromagnetic ordering,[57] even though neutron diffraction did not show the presence of a magnetic superlattice.[58] From the present work, and that an Al_2O_3,[56] it would appear that the magnetic hyperfine spectrum observed for ^{57}Fe in V_2O_3 is due to spin-lattice alignment and not to magnetic ordering.

In $NaSc_{1-x}Fe_xTiO_4$ and other isomorphous series studied in the present work, the $g' = 4{\cdot}3$ signal was replaced by a $g' = 2$ signal when approximately 0·10 of the total number of octahedral or tetrahedral sites were occupied by Fe^{3+}. At this concentration the occurrence of Fe^{3+} pairs becomes strongly probable, and coupling between such pairs produces ground-state energy levels

[50] J. E. Bennett, J. F. Gibson, and D. J. E. Ingram, *Proc. Roy. Soc.*, 1957, *A*240, 67.
[51] J. S. Griffith, *Proc. Roy. Soc.*, 1956, *A*235, 23.
[52] D. M. Hannon, *Phys. Rev.*, 1967, **164**, 366.
[53] G. G. Wepfer and C. Kikuchi, *Phys. Rev.*, 1968, **170**, 445.
[54] (*a*) E. S. Kirkpatrick, K. A. Müller, and R. S. Rubins, *Phys Rev.*, 1964, **135**, *A*86; (*b*) R. Baer and G. Wessel, *J. Appl. Phys.*, 1968, **39**, 23.
[55] D. L. Carter and A. Okaya, *Phys. Rev.*, 1960, **118**, 1485.
[56] G. K. Wertheim and J. P. Remeika, *Phys. Letters*, 1964, **10**, 14.
[57] T. Shinjo, K. Kosuge, M. Shiga, Y. Nakamura, S. Kachi, and H. Takaki, *Phys. Letters*, 1965, **19**, 91.
[58] A. Paoletti and S. J. Pickart, *J. Chem. Phys.*, 1960, **32**, 308.

which are to good approximation independent of the crystal field and give rise to $g' = 2$ e.s.r. signals.[1] The interaction which allows this coupling, transmitted by way of the oxygen atoms bonding one Fe^{3+} to another, or to intermediate Sc or Ti atoms, is one to which the Mössbauer effect is evidently very sensitive, since the magnetic spectrum disappears at Fe^{3+} concentrations much lower than those which cause the $g' = 4{\cdot}3$ e.s.r. signal to be removed. The alignment of the spins of isolated Fe^{3+} ions with respect to the crystal field can evidently be upset by interactions which extend not merely to the nearest-neighbour metal-atom site, but to Fe^{3+} ions several sites away. A comparable interaction was observed [59] by Goldanskii and Belov *et al.* for diamagnetic Sn atoms introduced into yttrium iron garnets $(Y_{3-x}Ca_x)(Sn_xFe_{2-x})Fe_3O_{12}$. In these compounds a magnetic field of 200 kgauss was observed at the Sn nuclei as a result of Fe–O–Sn superexchange. More distant superexchange is conceivable in the present oxide compounds, since like ions are interacting, and co-operative phenomena should be enhanced.

It is noteworthy that there appears to be no correlation between average environmental bond length for Fe^{3+} sites (Table 1) and parameters such as quadrupole splitting. Evidently local site symmetries, local crystal fields, and superexchange effects are more important. Furthermore, individual Fe^{3+} ions will usually tend to distort their local sites to attain suitable average bond-lengths.

We are at present studying low concentrations of Fe^{3+} in cubic crystals, and those with local axial fields, such as $SrTiO_3$ and TiO_2, since there seems no reason to suppose that spin alignment with respect to the crystal field axes cannot occur in such host lattices, especially at temperatures at which rapid realignment among equally preferred crystalline directions can be prevented. In a comparable system, 5% of iron in solid solution in gold, a strictly cubic lattice, a magnetic ordering of spins (shown to be antiferromagnetic) occurs, with a characteristic six-line magnetic spectrum being produced.[60,61] In the $Au_{0{\cdot}95}Fe_{0{\cdot}05}$ system interaction of the unpaired electrons takes place by way of the conduction electrons rather than through metal–oxygen bonds as in oxide host lattices.

In the present series of compounds we have also examined the electronic transition spectra as a function of Fe^{3+} concentration, since it was previously found for the $NaSc_{1-x}Fe_xTiO_4$ system [1] that marked changes in optical spectra accompanied the changes in the e.s.r. absorptions. The optical absorptions corresponding to a given electronic transition are remarkably constant in position from compound to compound, although, as expected, the transitions to the two lowest levels $^4T_1(^4G)$ and $^4T_2(^4G)$, whose energies are crystal-field dependent, do show a significant frequency variation. In all cases the spectra can be assigned on the same basis as for $NaSc_{1-x}Fe_xTiO_4$,[1] and in the present work the spectra of $NaSc_{1-x}Fe_xO_2$ were found to show all six of the transitions possible up to 40,000 cm.$^{-1}$, and to exemplify the spectrum of an Fe^{3+} ion in an oxide host lattice. The assignment given in Table 5 is based on the energy matrices of Tanabe and Sugano,[62] using the same constants as used for $NaSc_{1-x}Fe_xTiO_4$, namely $10Dq = 13{,}300$; $B = 900$ cm.$^{-1}$; $C/B = 4{\cdot}0$, and allowing a change in the centre of gravity of the set of excited levels with respect to the ground state level of 6300 cm.$^{-1}$ to allow for covalence.[63] This centre of gravity shift is obtained by identifying the $^4A_1$, $^4E(^4G)$ transition at 20,700 cm.$^{-1}$, at which value it appears with remarkable constancy for all the systems studied, and comparing this with the free-ion value of 27,000 cm.$^{-1}$.

As expected for a $3d^5$ system, the transitions conform to the same set of quartet levels predicted for Mn^{2+}, as shown in the ligand-field diagrams of Orgel,[64] with appropriate changes in the energies and separations of the levels. Transitions derived from the ^4F free-ion term are not observed in any of the present spectra of octahedrally co-ordinated Fe^{3+}, but in β-$NaAl_{1-x}Fe_xO_2$ tetrahedrally co-ordinated Fe^{3+} in a rather distorted tetrahedron appears to exhibit a transition to the $^4A_2(^4F)$ level, and probably to the $^4T_1(^4F)$ level as well, since a strong but unresolved absorption occurs in the region above 40,000 cm.$^{-1}$.

Despite the constancy of the positions of those bands which do appear in the range of host lattices studied, the relative intensities of the six levels derived from the ^4G, ^4P, and ^4D free-ion terms varies considerably. For a d^5 system all transitions are to first approximation forbidden, and we can indeed expect a considerable variation in intensities with the strength and anisotropy of the crystal fields in the various host lattices.

In $NaSc_{1-x}Fe_xTiO_4$, as previously described,[1] the ^4E (^4D) transition was strong for isolated Fe^{3+}, but disappeared when Fe^{3+} pair effects became dominant. At the same time the $^4T_2$ (^4D) band, absent at first, increased in intensity to become very strong at higher concentrations. We see in the present work that this was a peculiarity of the $NaSc_{1-x}Fe_xTiO_4$ system, and that both of these transitions are generally strong. We can note that the two lowest energy Dq-dependent bands at 9600 cm.$^{-1}$ and 15,500 cm.$^{-1}$ are always absent or of very low intensity for low Fe^{3+} concentrations and increase slowly, while the intensity of the sharp transition to the ^4A, ^4E (^4G) level increases approximately linearly with concentration. For octahedral Fe^{3+}, transition to $^4T_2$ (^4D) is always the most intense, with ^4E (^4D) usually of comparable intensity, but occasionally absent as in $NaFeTi_3O_8$.

The effect of host lattice absorption can be pronounced if an isomorphous reference compound is not used, as can be deduced from Figures 7 and 11, for

[59] V. I. Goldanskii, *Angew. Chem. Internat. Edn.*, 1967, **6**, 830.
[60] R. J. Borg, R. Booth, and C. E. Violet, *Phys. Rev. Letters*, 1963, **11**, 464.
[61] P. P. Craig and W. A. Steyer, *Phys. Rev. Letters*, 1964, **13**, 802.
[62] Y. Tanabe and S. Sugano, *J. Phys. Soc. Japan*, 1954, **9**, 499.
[63] D. S. McClure, *Solid State Phys.*, 1959, **9**, 499.
[64] L. E. Orgel, *J. Chem. Phys.*, 1955, **23**, 1004.

example. The absorption of the iron-free titanate host lattice is strong in the u.v. region, falling to an absorption edge just before the visible, at *ca.* 29,000 cm.$^{-1}$ (Figure 7). When an Fe^{3+} spectrum is recorded with MgO as the reference substance, the lattice absorption adds to that of the Fe^{3+} ion and obscures bands above about 20,000 cm.$^{-1}$. Host lattice absorption is much less for $NaScO_2$ and β-$NaAlO_2$, but in all cases, as expected for a double-beam spectrophotometric arrangement, a sample of the host lattice *vs.* the host lattice as reference demonstrates almost complete cancellation of the host lattice absorption. We can therefore be confident that the absorptions observed in the present work are crystal field bands of Fe^{3+}, and the consistency of their positions regardless of whether the host lattice is a strong absorber like $Cs_xSc_xTi_{2-x}O_4$ (Figure 11) or a weak absorber like $NaScO_2$ (Figure 7) confirms this expectation.

We are greatly indebted to Dr. F. D. Looney and Dr. I. A. Campbell of the Division of Applied Chemistry, and Division of Chemical Physics, C.S.I.R.O., for recording the e.s.r. spectra. We thank the S.R.C. for financial support and the award of a postdoctoral fellowship to T. B.

[8/1821 *Received, December* 10*th*, 1968]